38th AIAA/ASME/SAE/ASEE Joint Propulsion Conference & Exhibit
7-10 July 2002, Indianapolis, Indiana

AIAA 2002-4029

CHARACTERIZATION OF PINTLE ENGINE PERFORMANCE FOR NONTOXIC HYPERGOLIC BIPROPELLANTS

Austin, B. L.* and Heister, S. D.†
School of Aeronautics and Astronautics, Purdue University
West Lafayette, IN 47906

Abstract

Using rocket grade hydrogen peroxide (RGHP) and a nontoxic, hypergolic miscible fuel (NHMF), a 150-lbf thrust class pintle injector engine has been developed at Purdue University for the purposes of determining parameters leading to high combustion efficiency. The parameters investigated include characteristic length, chamber diameter-to-pintle diameter ratio, total momentum ratio (TMR), secondary-to-primary hole diameter ratio, and the pintle length-to-pintle diameter ratio. High performance has been achieved in both steady-state and pulse mode operation.

Nomenclature

RGHP	Rocket grade hydrogen peroxide
NHMF	Nontoxic, Hypergolic, Miscible Fuel
TMR	Total Momentum Ratio
NTO	Nitrogen tetroxide
MMH	Monomethyl hydrazine
TMR	Total Momentum Ratio
I_{SP}	Specific impulse
I_{SPv}	Vacuum Specific Impulse
ρI_{SPv}	Vacuum density specific impulse
P_C	Chamber pressure
ϵ	Nozzle area ratio
D_{SEC}	Secondary hole diameter
D_{PRI}	Primary hole diameter
L*	Characteristic length
c*	Characteristic velocity
sps	Samples per second
fps	Frames per second

Introduction

The current standard in high-performing, storable bipropellants is the combination of nitrogen tetroxide (NTO) and monomethyl hydrazine (MMH). In addition to delivering high levels of specific impulse (I_{SP}), the propellants are hypergolic, which greatly simplifies engine design and operation. However, both nitrogen tetroxide and the hydrazine-based fuels (hydrazine, MMH, unsymmetrical dimethyl hydrazine, aerozine-50) pose serious health hazards. Nitrogen tetroxide has an exposure limit of 5-ppm but a very high vapor pressure of 720-mmHg.[1] MMH, a carcinogenic liquid, has a relatively low vapor pressure of 36-mmHg but a personal exposure limit of 200-ppb.[1] Material Safety Data Sheets specify the use of respirators in addition to full body acid/chemical impermeable protection when handling these propellants. Furthermore, NTO requires rinse showering after handling. Given these handling requirements as well as the extensive equipment, monitoring, and regulation necessary to ensure safe storage and use of the propellants, considerable effort has recently been put forth in investigating low or nontoxic alternative propellants with high performance.

In 1993, the Naval Air Warfare Center Weapons Division (NAWCWD) at China Lake began searching for nontoxic propellants for use in divert and attitude control engines on ship-based ballistic missile defense intercept missiles.[2] By 1997, NAWCWD researchers had developed a class of storable, nontoxic fuels that were hypergolic with and completely miscible in rocket grade hydrogen peroxide. The first of these NHMFs, Block 0, is a catalyzed methanol, which approaches 93% of the vacuum specific impulse (I_{SPv}) and 99% of the vacuum density specific impulse (ρI_{SPv}) of NTO/MMH when used with 98% hydrogen peroxide. Theoretical performance data of these two sets of bipropellants are shown in Figure 1.[3] New formulations of nontoxic fuels under development at Purdue University and Swift Enterprises, Ltd. have theoretical vacuum specific impulses greater than 95% of NTO/MMH and density vacuum specific impulses that meet or exceed the NTO/MMH values.[3,4]

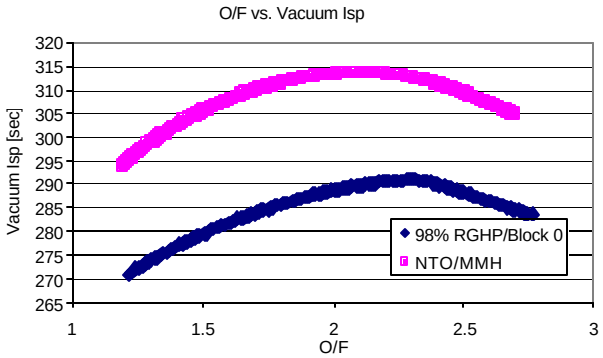

Figure 1: Performance comparison of NTO/MMH and RGHP/NHMF propellants. (P_C = 500-psia, ϵ = 10)

* Graduate Student, Student Member AIAA
† Professor, Associate Fellow AIAA

Additional work has focused on ignition delay determination of the RGHP/NHMF propellants.[3,5] This property is of significant interest since the kinetic kill vehicle application is particularly sensitive to the length of time required to reach full thrust. The ignition delay of RGHP/NHMF is approximately 15-msec, which is roughly comparable to the 2-msec ignition delay of NTO/MMH using the same drop tester.[5]

To further the use of the RGHP and NHMF propellants in divert and attitude control engines on a kinetic kill vehicle, experimental determination of engine parameters leading to high performance have been investigated in the current research. A pintle injector was selected for the workhorse engine based on its relative ease of manufacturing, inherent stability, and to support parallel efforts underway at KB Sciences.[6]

Test Apparatus

Engine

A 200-lbf vacuum thrust pintle engine with a 400-psia chamber pressure was designed and fabricated. The engine was designed to be modular in order to allow changes to the various geometries affecting the parameters of interest without constructing time-consuming and costly new engines for each parameter. Additionally, if part of the engine sustained damage from over-pressurization or ablation, the component could be replaced without having to reconstruct large engine components. A drawing of the baseline pintle engine is shown in Figure 1.

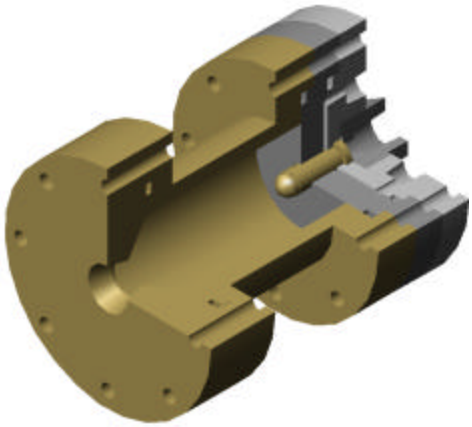

Figure 2: Cutaway view of modular pintle engine.

Fuel passes through the top of the pintle injector plate and continues straight into a central post extending through the annulus injector plate and into the chamber. The pintle post sprays the fuel radially into the chamber through holes located near the tip of the post. The RGHP flows into two ports passing through the pintle injector plate and is guided in the direction of the central post through two channels in-between the fuel and oxidizer manifold plates. The oxidizer turns 90° towards the chamber when it reaches the post and passes through a small (nominally 0.022-in) gap creating a cylindrical liquid sheet, or annulus, which flows down the pintle post. The fuel and oxidizer flows intersect and begin mixing at the fuel exit orifices around the pintle post. Since hypergolic propellants do not require an additional source of ignition, combustion initiates a short distance away from the post.

The pintles used in this study all consisted of two rows of equally spaced, circular holes; a row of primary holes, larger and closer to the annulus injector, and a row of secondary holes, smaller and closer to the pintle tip. A secondary hole diameter, D_{SEC}, of 0.0150-in was chosen as a nominal value since this was the smallest hole size that the machining facility could reliably and quickly drill. The primary hole diameter, D_{PRI}, was select to be 0.0228-in in the baseline design. To reduce the number of design variables, only cases with equal number of secondary and primary holes were considered for this research. For a 0.375-in diameter pintle, 16 primary/secondary hole pairs were used to achieve a Blockage Factor, the fraction of the pintle's exterior surface that is taken up by injector orifices as seen from the annulus injector, of 0.5. In previous papers, pintles are generally shown to have a flat exterior tip with an insert used to turn the flow radially. However, pintles used in this study had hemispherical exterior and interior tips. The rounded exterior was to prevent a flame from attaching to the pintle and causing heat damage. The hemispherical interior was used to allow the fuel flowing through the pintle to absorb the heat energy.

For the engine size selected, a fuel-center pintle was preferred over oxidizer-centered for several reasons. Previous engines using RGHP and NHMF propellants noted a hard-start when the oxidizer preceded the fuel into the chamber. With the planned injector layouts, the annulus injector required a larger fill volume, thus, flowing oxidizer through the annulus would result in a fuel lead. Additionally, injecting fuel through the annulus at the desired velocity required a 0.0033-in gap between the pintle and annulus wall. Given the ±0.0005-in machining tolerances available, the variance in the fuel injection velocity could be upwards of 30%. With the oxidizer having a mass flow rate almost three times that of the fuel, the machining tolerances were much less significant. Finally, for high fuel velocities, it was hypothesized that the fuel jets would penetrate the oxidizer annulus resulting in a cooler, fuel rich region near the chamber wall.

The engine is composed of stainless steel pintle and annulus injector/manifold plates, a copper chamber with a characteristic length of 29.6-in, and a copper nozzle plate. Stainless steel pintles were used because copper and Aluminum 6061-T6 pintles would either break or elongate at the primary row of holes under the pressure and heat loads. A combustion chamber wall thickness of 0.25-in provided a safety factor of 1.25 over the yielding stress of the standard Grade 2 bolts used to fasten the injector plates, chamber, and nozzle together. This allowed the chamber to separate from the injector plates or nozzle prior to the chamber wall breeching in the event of over-pressurization. Table 1 is a summary of the relative pintle engine information. Complete engine details are available through the authors.

Table 1: Baseline engine design.

General		
Chamber Pressure	400	psia
Vacuum Thrust	149	lbf
Vacuum Specific Impulse	231	sec
Characteristic Velocity	5159	ft/sec
Characteristic Length	29.6	in
Mass Flow Rates		
Total	0.643	lbm/sec
Oxidizer	0.471	lbm/sec
Fuel	0.172	lbm/sec
Mixture Ratio	2.74	
Pintle		
Pintle Diameter	0.375	in
Pintle Length	0.450	in
Primary Hole Diameter	0.0228	in
Secondary Hole Diameter	0.0150	in
Number of Hole Pairs	16	
Fuel Exit Area	0.00936	in^2
Fuel Injection Velocity	47.1	ft/sec
Annulus		
Injector Face Hole Diameter	0.418	in
Gap Distance	0.022	in
Oxidizer Exit Area	0.0268	in^2
Oxidizer Injection Velocity	28.4	ft/sec
Chamber		
Chamber Diameter	1.7460	in
Chamber Length	3.0015	in
Nozzle		
Throat Diameter	0.5690	in
Throat Area	0.254	in^2
Contraction Ratio	9.42	
Exit Diameter	0.7625	in
Exit Area	0.457	in^2
Expansion Ratio	1.799	

Test Stand

All pintle engine tests were conducted on the 1000-lb_f test stand located at Purdue University's Maurice Zucrow Laboratories. With a moveable thrust flexure, solid motors and hybrid, monopropellant, and bipropellant engines which use hydrogen peroxide as the oxidizer can be fired with minor adjustments. The test stand has a 4-gal hydrogen peroxide run tank as well as a 1-gal run tank for hydrocarbon fuels. Propellants are vacuum loaded into the run tanks, which can then be pressurized up to 1600-psia with gaseous nitrogen. Helium pressurized, pneumatic ball valves are used for all propellant lines to provide fast response with minimal pressure loss.

The data acquisition system used during test fires is capable of recording 1000-sps at 16-bit resolution. Standard instrumentation at the rocket lab consists of a 1000-lb_f Interface load cell, 1000-psia and 3000-psia Druck pressure transducers, Omega k-type thermocouples, differential pressure transducers, and v-cone flow meters. Other instrumentation devices such as accelerometers and heat flux gauges have also been used. Currently, there are 20 pressure transducers and 13 thermocouples wired into the National Instruments SCXI module, but 75 additional 0 – 5-Volt instruments and 16 thermocouples can be added.

Testing Results

Once the engine hardware was fabricated, water flow tests were performed to provide visualization of the propellant flow as well as to leak check the test stand and engine plumbing. Following the water flow tests, the RGHP and NHMF propellants were tested in the engine with the nozzle plate removed. These open chamber tests served to determine the propellant injection times and verify hypergolic ignition without risking an over-pressurization, which could harm the engine or test stand.

The first full engine test failed due to an over-pressurization resulting from the fuel reaching the chamber approximately 0.33-sec before the oxidizer. The second full engine test also resulted in an over-pressurization when a slight oxidizer lead was achieved. In both incidents, the engine failed at the intended point, the bolts holding the chamber onto the injectors. Engine damage was light and repairs were completed within a few hours.

The pintle engine was successfully fired for a 3-sec test on the third full engine attempt in July 2001. After cooling for a couple of minutes, two more 3-sec tests were conducted. Tank ullage pressures, injector pressures, mass flow rates and engine thrust data were acquired on all tests. The chamber pressure transducer failed midway into the second test so no chamber information was available form the third test. Post-test inspection of the engine components, including the pintle and nozzle throat, revealed no signs of erosion or wear.

Since July 2001, the pintle engine has been successfully fired over 150 times in 3-sec duration tests. An image of one of the test fires is shown in Figure 3. Some of these tests were conducted to verify experimental performance of six additional NHMFs under development at Purdue. Further tests were performed with varying mixture ratios of RGHP and Block 0. The remainder of the test firings were conducted to examine pulse duty cycles and investigate the parametric conditions discussed below.

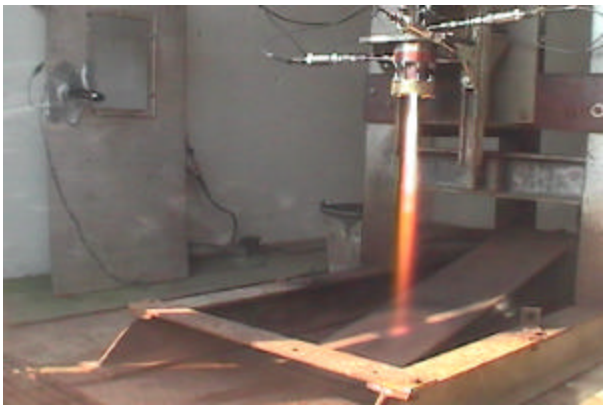

Figure 3: Test fire of pintle engine on Purdue's 1000-lbf test stand.

Typical unfiltered chamber pressure data, like that displayed in Figure 4, has shown that there is no overshoot evident in the chamber pressure pointing to a smooth startup. An overlay of two chamber pressure traces, shown in Figure 5, from two different test fires show that the pressures rise at the same rate to approximately the same point with little or no overshoot. This indicates that the ignition process is smooth, repeatable, and reproducible. The chamber pressure reaches 90% of the steady state level within 80-msec.

Usual variance in the chamber pressure signal is approximately ±10% of the steady state signal indicating that the combustion is somewhat rough. A splash plate engine using the same propellants, mass flow rates, chamber and nozzle has demonstrated a chamber pressure variation of only ±4%.[7] Despite taking considerable means to tighten the nut securing the pintle into the injector plate, the pintle post can be moved slightly towards the annulus wall by applying a moderate amount of pressure to the side of the pintle. Given this and the low noise in the splash plate engine, it is postulated that the combustion roughness in the pintle engine test is the result of the pintle vibrating about the engine centerline due to pressure variations inside the chamber.

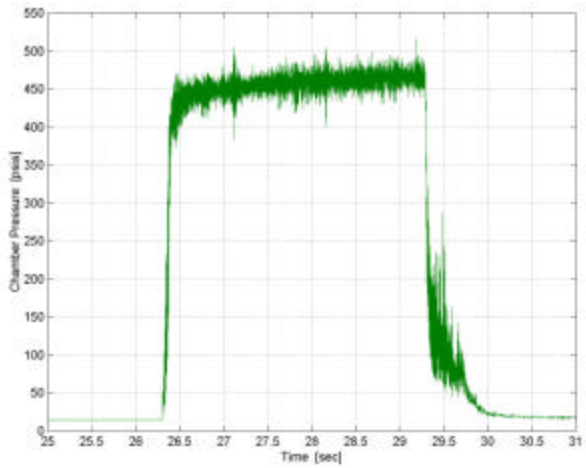

Figure 4: Chamber pressure vs. time for a 3-sec test.

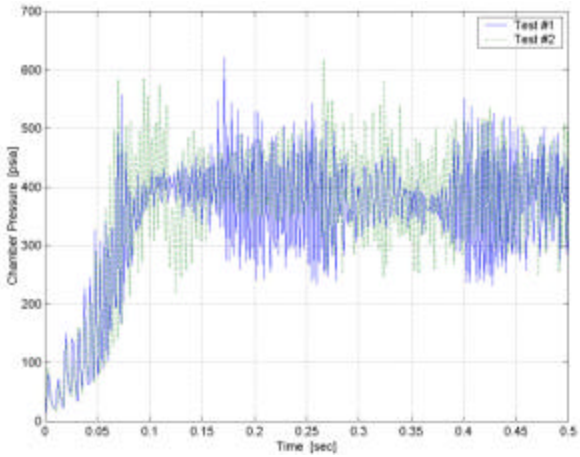

Figure 5: Overlay of two unfiltered chamber pressure traces from two different test fires.

The Fast Fourier Transform of the chamber pressure data in Figure 4 is shown in Figure 6 with the y-axis scale amplified 36 times; the steady state signal has a magnitude of over 90 on this graph. The FFT shows little organized frequency activity between 0-Hz and 500-Hz. The estimated L1 and T1 instability frequencies are orders of magnitude higher than the current 1000-sps data sampling rate can resolve. However, audible noise levels during the test fires do not indicate an instability.

The thrust data for the test shown in Figure 4 is shown in Figure 7. The thrust levels trace the chamber pressure and are also repeatable in terms of thrust level, rise times, and startup and shutdown transients. Further, the variation in the thrust signal is about the same percentage as the variation in the chamber pressure.

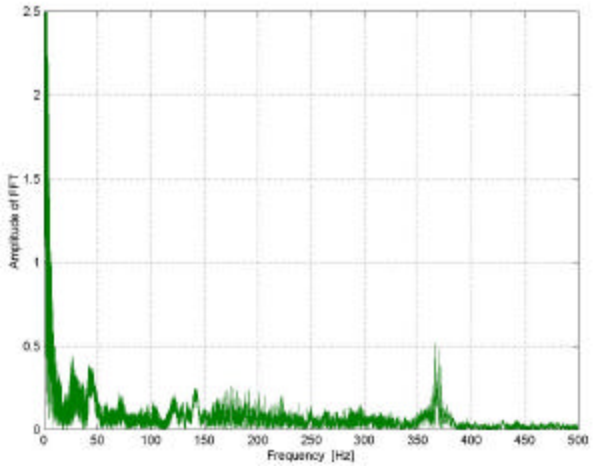

Figure 6: FFT of chamber pressure (with scale amplified 36 times).

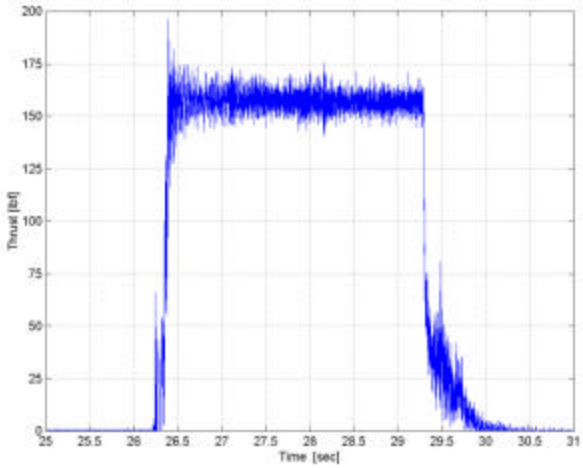

Figure 7: Thrust vs. time for a 3-sec test.

To provide a degree of accuracy in the measured data and calculated results, the error analysis methodology outlined by Cahill et al[8] was employed. Lacking pressure and force standards, end-to-end calibrations of the pressure transducers and load cell could not be performed. However, estimates for the bias error were made based on information supplied by the instrumentation manufacturers. Using this methodology and these approximations, the errors in the c* efficiency and specific impulse were estimated to be approximately ±2.3% and ±5-sec, respectively.

Since the pintle engine was being developed for use as a divert engine, rapid succession, short duration tests were conducted to simulate the engine in such a duty cycle. The LabVIEW program used to command the valves sent signals in minimum intervals of 0.10-sec. This meant that pulse tests could not be performed faster than 0.10-sec ON/0.10-sec OFF. To ensure ignition would take place during the short duration, a single 0.10-sec duration test was executed. Following that success, one 5-pulse and two 11-pulse tests were conducted. The chamber pressure trace of an 11-pulse test is shown in Figure 8. The thrust signal clearly indicates 11 pulses with only the first one being significantly lower than the rest. The first pulse in the set is expected to be lower than the rest considering that the feed lines are clear before that pulse and relatively full for all of the others. While this testing demonstrated pulse-to-pulse repeatability, the valving and manifolding used in the facility are not optimal to truly test the minimum pulse widths achievable with this system.

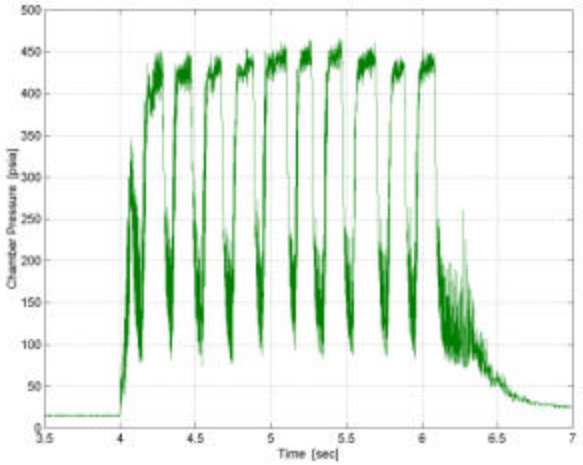

Figure 8: Chamber pressure vs. time for pulse test with 11 0.1-sec ON/0.1-sec OFF cycles.

An acrylic chamber was constructed and fired in an attempt to see the startup transient and initial flow patterns. An image from the 6-sec firing is shown in Figure 9. While the ignition event was not captured by the 60-fps camera, post-test analysis of the chamber interior showed that the wall receded uniformly by approximately 0.25-in with the exception of 16 small locations (approximately 0.25-in in diameter), which showed about a 0.08-in of recession, 0.48-in down from the chamber headend. This evidence combined with the close-up video in Figure 10 showing fuel impacting the chamber wall verifies that, for a chamber diameter of 1.75-in and a fuel injection velocity of 47.1-ft/sec, the fuel exiting the primary pintle holes penetrates the oxidizer flow and cools the chamber wall directly opposite the injection locale.

Figure 9: Test firing with acrylic chamber.

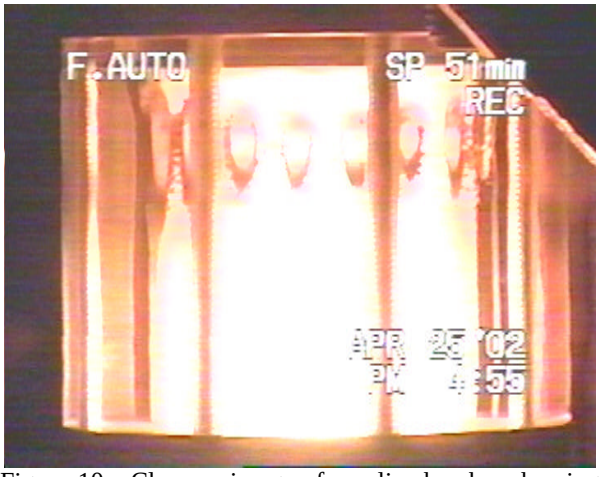

Figure 10: Close-up image of acrylic chamber showing radial fuel jet impact points on the outer chamber wall.

Steady State Parametric Test Results

Once testing reached the point of consistently and reliably providing data, parametric studies were initiated. Each parameter was tested in two 3-sec fires resulting in 60 steady state tests. The characteristic length and narrow and wide chamber TMR tests were also tested in a total of 37 pulse tests. The following sections detail the results from the parametric tests. All c* efficiencies are based on a one-dimensional, equilibrium, theoretical characteristic velocity of 5159-ft/sec obtained from the Air Force I_{SP} Code. Many of the c* efficiencies reported in the following parametric studies are at or above 100%. This is likely a result of error sources such as changes in the throat diameter due to thermal expansion, heat transfer to the chamber wall, and chamber pressure transducer placement not accounting for Rayleigh losses. Likewise, the measured specific impulses are above the theoretical maximum of 188-sec predicted by the Air Force I_{SP} Code. Given the substantial difference between the measured and theoretical values, it is believed that the load cell measuring the engine thrust is out of calibration. However, the results are presented here for comparison.

Characteristic Length

Given the modular design of the engine, the characteristic length was easily varied by using different combinations of three chamber sections. The c* efficiency and specific impulse increased as the engine's characteristic length increased as shown in Figure 11, indicating excellent combustion at L* values of 30 inches or greater. The general trend agrees well with theory since increasing L* increases the propellant residence time, therefore permitting the propellants more time to mix, evaporate and combust. While performance improved with L*, the characteristic length and, thus, chamber volume increasing by a factor of four had no discernable affect on the chamber pressure rise time.

Chamber Diameter-to-Pintle Diameter Ratio

Since changing the pintle diameter would alter the angular spacing between the pintle holes as well as the annulus injector area, the chamber diameter was varied to change the Chamber Diameter-to-Pintle Diameter Ratio. However, given the machining and testing time requirements, there was only enough time to test one Chamber Diameter-to-Pintle Diameter ratio beyond the baseline ratio. With the injector pattern and velocities, a wider chamber was more likely to result in higher combustion efficiency than a narrower one. The largest chamber diameter that could be used in the modular engine without risking damage to the o-rings was 2.25-in, thus, this size was constructed.

Since two points are an insufficient number on which to base a trend, no c* efficiency or I_{SP} graphs for this test series are presented though both test conditions are included in the Total Momentum Ratio studies (narrow and wide chambers) at the baseline TMR of 0.61. In comparing the data from these two tests, the average c* efficiency of the narrow chamber is 11.4% higher than that of the wide chamber. However, in comparing the specific impulses, the two tests are equivalent within the estimated error.

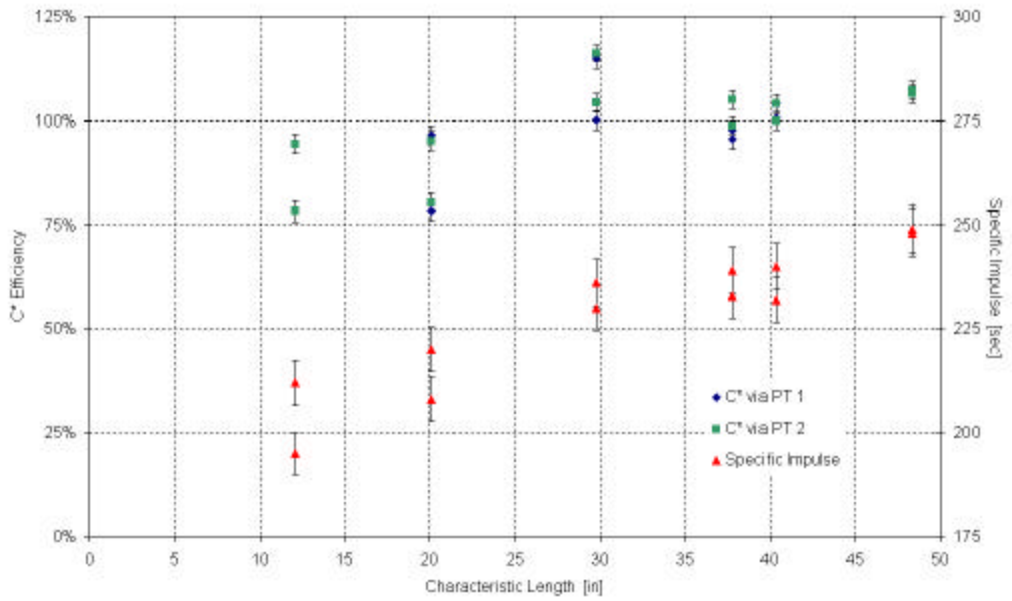

Figure 11: C* efficiency and I_{SP} vs. characteristic length.

Total Momentum Ratio

The total momentum ratio is defined as the momentum rate of the propellant flowing through the pintle divided by the momentum rate of the propellant flowing through the annulus. Given that changes in mass flow rates result in changes in chamber pressure or mixture ratio, the TMR study was performed by varying the fuel and oxidizer velocities while keeping the mass flow rates constant. Two additional pintles providing 24.1-ft/sec and 66.7-ft/sec fuel injection velocities and two additional oxidizer plates providing 17.7-ft/sec and 23.7-ft/sec oxidizer injection velocities were constructed. This permitted nine different TMR combinations ranging from 0.30 to 1.36 to be tested.

For the narrow chamber, the c* efficiency and I_{SP} graphs shown in Figure 12 have logarithmic shapes, which appear to asymptote at a TMR of approximately 0.7. When the lowest TMR for the narrow chamber was tested, the propellants initially ignited but were extinguished within 100-msec of the start of the chamber pressure rise. From the video, it appears that the peroxide continued to decompose, to an extent, for the remainder of the test. The c* efficiencies and specific impulses reported at this lower TMR are the values obtained at the beginning of the tests since the chamber did not achieve steady state operation.

Unlike the narrow chamber tests, the measured c* efficiency and I_{SP} of the TMR study done with the wide chamber are relatively insensitive to the TMR as seen in Figure 13. Additionally, there were no incidents of propellants extinguishing at even the lowest TMR conditions tested.

Secondary-to-Primary Hole Diameter Ratio

In an effort to isolate the hole diameter ratio study from the total momentum ratio, it was necessary to keep the fuel exit area as close as possible to the baseline case. However, this was limited by the drill bit sizes available from suppliers and the angular resolution of the equipment used to locate and drill the holes. The baseline secondary hole diameter of 0.0150-in was selected for all of the ratios (except for the D_{SEC}/D_{PRI} = 1.00 case where D_{SEC} = 0.0157-in). Primary hole diameters were calculated for an incremental number of primary/secondary hole pairs using the baseline exit area. The primary hole diameter and number of hole pairs were then selected based on which ones resulted in a "convenient" angular spacing.

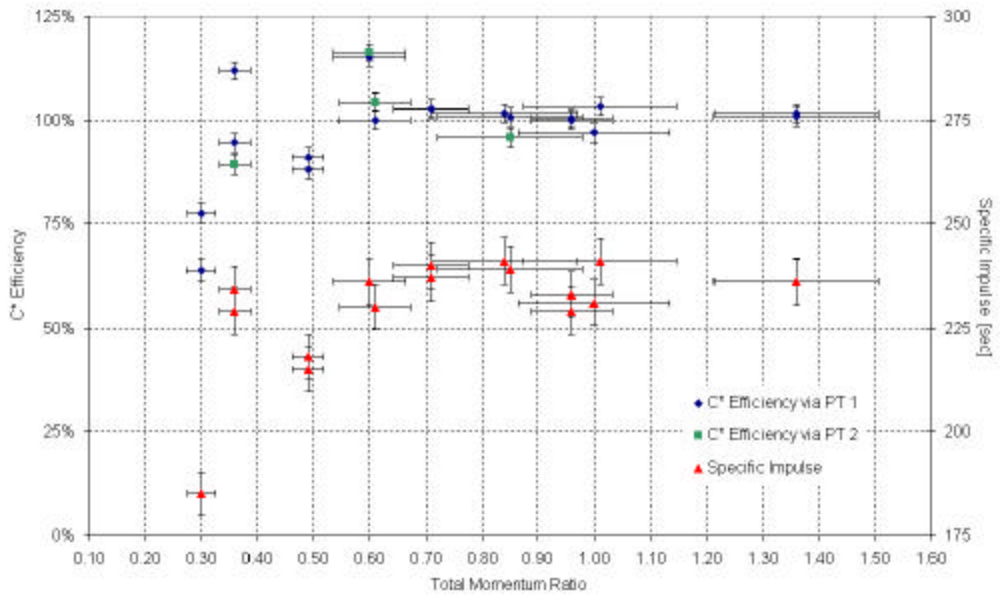

Figure 12: C* efficiency and I_{SP} vs. TMR with the 1.75-in diameter chamber.

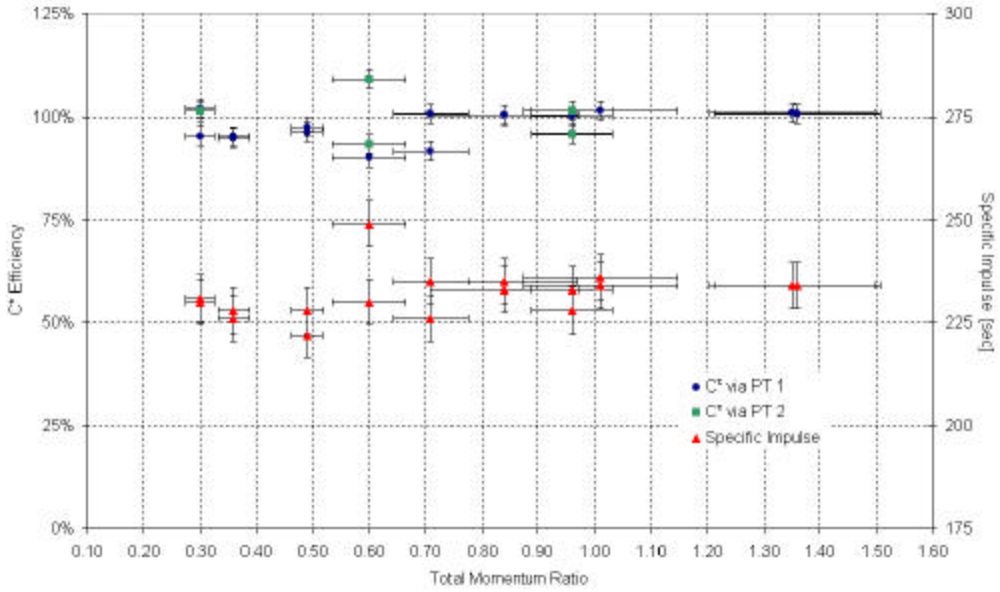

Figure 13: C* efficiency and ISP vs. TMR with the 2.25-in diameter chamber.

As shown in Figure 14, the c* efficiency decreases slightly as the Secondary-to-Primary Hole Diameter Ratio increases and the I_{SP} does not vary significantly outside of the estimated error. In typical liquid rocket engines, smaller injector orifices produce smaller propellant droplets, which, in general, lead to better combustion efficiency given that the time required to evaporate a drop increases with the square of the drop diameter. Since the characteristic velocity and specific impulse do not increase as the primary hole diameters decrease, the diameter of the drops formed in pintle injector engines must be determined by another parameter or there must be adequate residence time to evaporate and combust these larger drops. For reference, the TMR during the study was kept to within 0.01 of the 0.61 baseline test value, sufficiently isolating the Secondary-to-Primary Hole Diameter Ratio from the TMR studies.

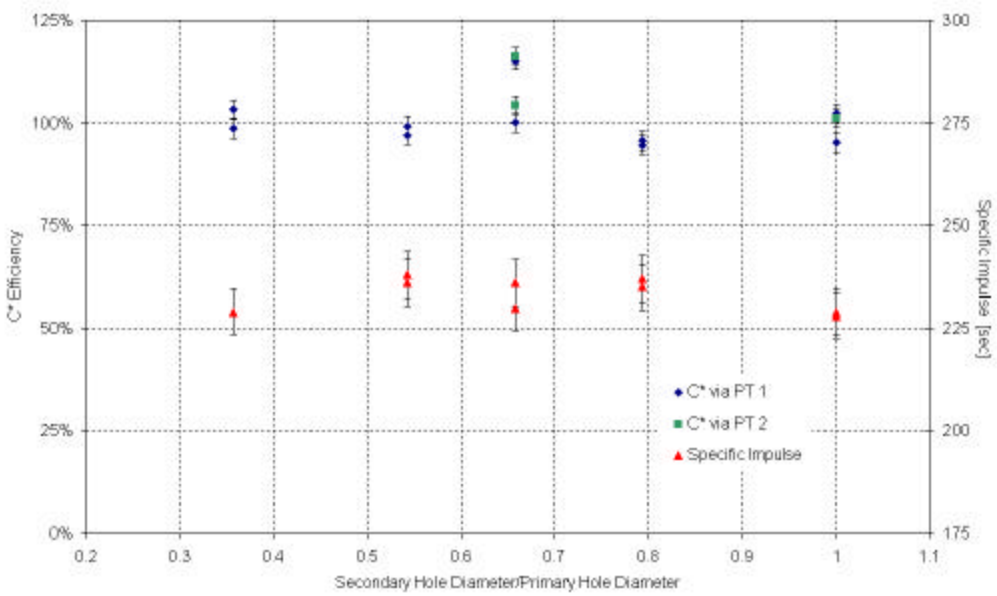

Figure 14: C* efficiency and ISP vs. Secondary-to-Primary Hole Diameter ratio.

Pintle Length-to-Pintle Diameter Ratio

For the same reasons mentioned in the Chamber Diameter-to-Pintle Diameter study, the pintle length was altered in order to vary the Pintle Length-to-Pintle Diameter ratio rather than changing the pintle diameter.

As seen in Figure 15, c* efficiency decreased by 5% and I_{SP} decreased by almost 11% when the pintle length was increased from 0.462-in to 1.262-in. This decrease is likely the result of the longer pintles causing the propellant residence time to decrease and less propellant to combust inside the chamber. Also noted during this test series was that the noise in the chamber pressure signal increased from about 12% of the steady state signal to as much as 37% as the pintle length increased. This observation supports the speculation that the combustion roughness is the result of the pintle oscillating about the centerline of the engine.

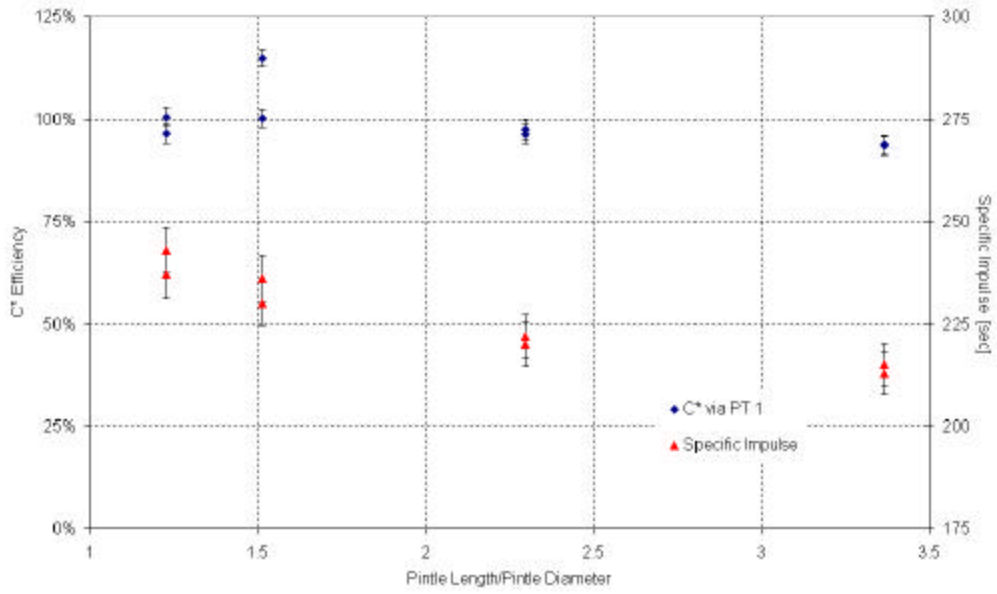

Figure 15: C* efficiency and I_{SP} vs. Pintle Length-to-Pintle Diameter ratio.

Pulse Mode Parametric Test Results

Pulse tests were conducted for the characteristic length and total momentum ratio tests. These tests followed the 11 0.1-sec ON/0.1-sec OFF cycles discussed above. The characteristic velocity efficiencies, specific impulses, and other statistical results presented are based on the last 10 of the 11 pulses since the lack of propellants in the feed lines leading up to the injector at the start of the pulse tests consistently lead to much lower performance of the first pulse than the remainder of the pulses.

Characteristic Velocity

The c* efficiency and specific impulse of each 0.1-sec pulse is shown in Figure 16 for each characteristic length tested. As is evident in the figures, the c* efficiencies and specific impulses increase as L* increases, the same trend observed in the 3-sec burn duration tests. In this case, it appears there is a benefit in increasing L* beyond 30 inches for optimal performance in a pulsing mode.

Total Momentum Ratio

Unlike the logarithmic shape of the performance curves of the 3-sec narrow chamber TMR tests, the c* efficiency and I_{SP} of the narrow chamber TMR pulse tests are relatively flat as seen in Figure 17. The fact that the lower TMR pulse tests have higher c* efficiencies and specific impulses than their 3-sec duration counterparts is believed to the consequence of the hydrogen peroxide having insufficient time to quench the combustion.

The c* efficiency and ISP of the TMR pulses tests with the wide chamber shown in Figure 18 appear very similar to the steady state performance.

Chamber Pressure Levels

A concern of pulse testing the pintle engine was that the engine be able to achieve repeatable and consistent chamber pressures. While each pulse being plotted on Figures 16 though 18 displays the amount of variation in the c* efficiencies and specific impulses of each test, the standard deviation in the chamber pressure for each pulse test was also determined. Most of the pulse tests had a standard deviation in the maximum chamber pressure of 15-psi or less.

While the chamber pressure during the ON portion of the pulse operation reach levels comparable to the steady state testing, the chamber pressures did not return to atmospheric between pulses. Since divert control of the engine would also depend on the chamber pressure and thrust between pulses, these values were also summarized. The average chamber pressure during the OFF portion of pulse testing was approximately 85-psia with minimums of 38-psia and maximums of 153-psi. There was approximately twice as much variation in the chamber pressure between pulses than there was in the chamber pressure during the pulses. The chamber pressures between pulses would be more consistent and lower (returning to ambient) with shorter propellant feed lines between the valves and the engine.

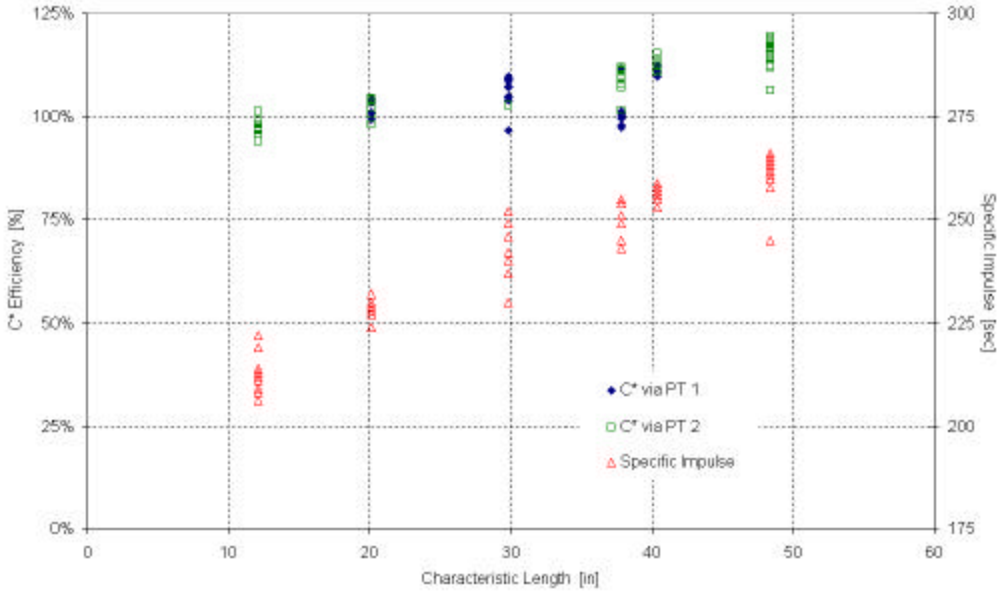

Figure 16: C* efficiency and I_{SP} vs. characteristic velocity for pulse tests.

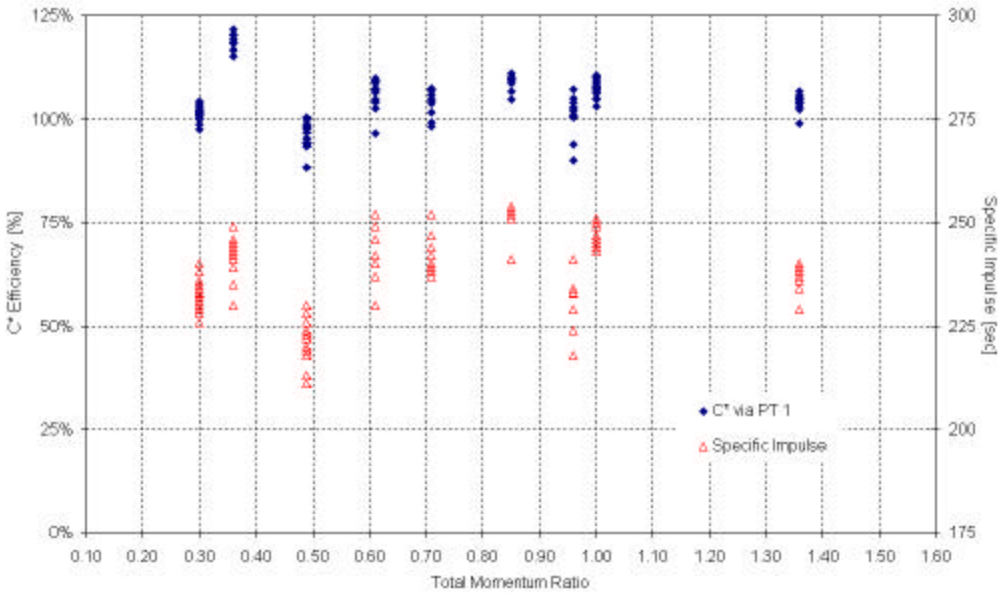

Figure 17: C* efficiency and I_{SP} vs. TMR with the ϕ1.75-in chamber for pulse tests.

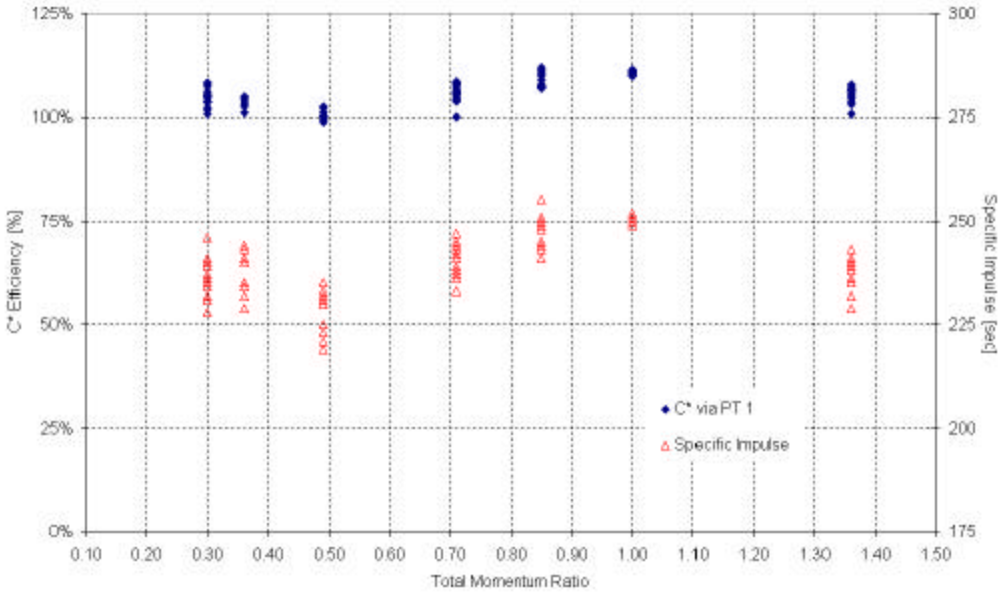

Figure 18: C* efficiency and I_{SP} vs. TMR with the ϕ2.25-in chamber for pulse tests.

Conclusions

A modular pintle engine has been fabricated and successfully tested with nontoxic hypergolic bipropellants based on hydrogen peroxide and a methanol fuel laced with catalyst. Rapid, reproducible ignition has been demonstrated with this propellant combination under both single and multiple pulse firings. Typical rise times are on the order of 80 msec under both single and multi-pulse conditions. While the combustion is somewhat rough, no organized frequency content was discernable in the chamber pressure measurements. Combustion roughness levels of about 10% are attributed to the modular nature of the engine in that the pintle post is subject to some vibration.

Parametric studies were conducted to identify the influence of total momentum ratio, L*, chamber diameter, pintle hole sizes, and pintle length. Steady-state combustion was optimized for L* values greater than 30 inches and TMR values greater than 0.7 for the

baseline 1.75 inch diameter chamber. Good performance was achieved over the 0.3-1.36 TMR range with the larger 2.25 inch diameter chamber. No distinct trends were evidenced on the range of pintle hole sizes tested and shorter pintles led to improved performance. The testing of a transparent 1.75 inch diameter chamber showed fuel spokes impinging on the chamber wall at nominal TMR conditions.

Excellent performance under pulsing conditions was also demonstrated, although there is evidence that slightly larger L* values would be required to optimize c* for pulsed operation. There were no distinct effects of TMR on performance under pulsing conditions.

Acknowledgements

The authors would like to thank

- Ron Humble of KB Sciences for funding the research efforts under a Phase II SBIR with BMDO/NAWC.
- Scott Meyer of Purdue University for his immense help in improving engine testing,
- the AAE Machine Shop for their quality fabrication of engine components, and
- the propulsion students of the School of Aeronautics and Astronautics who aided in the many tests conducted.

References

1. Chemical Sampling Information, [On Line] Available: http://www.osha-slc.gov/dts/chemicalsampling/toc/toc_chemsamp.html
2. Meadem C.J., Lormand, B.M., Purcell, N.L. "Status of Non-Toxic Hypergolic Miscible Fuel Development at NAWCWD China Lake" 2nd International Hydrogen Peroxide Propulsion Conference, Nov 7-10, 1999, Purdue University, W. Lafayette, IN.
3. Palmer, R.K. Development and Testing of Nontoxic, Hypergolic Miscible Fuels. Masters Thesis, School of Aeronautics and Astronautics, Purdue University.
4. Pourpoint, T.L., Rusek, J.J. "Investigation of Homogeneous and Heterogeneous Catalysis for the Propulsive Decomposition of Hydrogen Peroxide". International Conference on Green Propellant for Space Travel, June 20-22, 2001. ESTEC, Noordwijk, The Netherlands.
5. Frolik, S. Hypergolic Liquid Fuels for use with Rocket Grade Hydrogen Peroxide. Masters Thesis, School of Aeronautics and Astronautics, Purdue University.
6. Humble, R.W. "Bipropellant Engine Development Using Hydrogen Peroxide and a Hypergolic Fuel". AIAA 2000-3554.
7. Austin, B.L., Matthews, J.B., Heister, S.D. "Engine/Injector Development for New Nontoxic Storable Bipropellants",13th Annual Propulsion Engineering Research Symposium, Huntsville, AL, October, 2001.
8. Cahill, David M. et al. "Assessment of Wind Tunnel Data Uncertainty". AIAA S-071-1995.